

## Article

# A Comparison of Volatile Organic Compounds in *Puerariae Lobatae Radix* and *Puerariae Thomsonii Radix* Using Gas Chromatography–Ion Migration Spectrometry

Yingchao Mao <sup>1,†</sup>, Lingfeng Zhu <sup>1,†</sup>, Fuhua Fu <sup>1</sup>, Lijun Zhu <sup>2</sup>, Jiajing Chen <sup>2</sup>, Jing Liu <sup>2</sup>, Dan Huang <sup>2,\*</sup>   
and Chang Lei <sup>2,\*</sup>

<sup>1</sup> Hunan Agricultural Product Processing Institute, Hunan Academy of Agricultural Sciences, Changsha 410125, China; mycjgs@hunaas.cn (Y.M.); zhulingfeng1988@163.com (L.Z.); fhfu686@163.com (F.F.)

<sup>2</sup> State Key Laboratory of Chinese Medicine Powder and Medicine Innovation in Hunan (Incubation), Science and Technology Innovation Center, Hunan University of Chinese Medicine, Changsha 410208, China; 202104030124@stu.hnucm.edu.cn (L.Z.); cjj02761118@163.com (J.C.); liushuishui@stu.hnucm.edu.cn (J.L.)

\* Correspondence: huangdan110@hnucm.edu.cn (D.H.); leichang@hnucm.edu.cn (C.L.)

† These authors contributed equally to this work.

**Abstract:** *Puerariae Radix* is one of the most widely used ancient traditional Chinese medicines and is also consumed as food, which has rich edible and medicinal value. *Puerariae Radix* can be divided into *Puerariae Lobatae Radix* (PL) and *Puerariae Thomsonii Radix* (PT). These two medicinal materials are very similar, and they are often mixed up or misused. In this study, gas chromatography–ion migration spectrometry (GC-IMS) was used to analyze the volatile organic compounds (VOCs) of PL and PT, and the differences in VOCs were analyzed using fingerprint, principal component analysis (PCA), and orthogonal partial least squares discriminant analysis (OPLS-DA). The results showed that a total of 173 VOCs were obtained from PL and PT, and 149 were qualitatively identified, including 38 aldehydes, 22 alcohols, 22 ketones, 19 esters, 13 esters, 10 acids, 10 pyrazines, 6 terpenes, 4 furans, and 2 pyridines. The characteristic VOCs of PL and PT were clarified by constructing GC-IMS fingerprints. PL and PT can be effectively distinguished, and five characteristic VOCs were screened using PCA and OPLS-DA analysis methods. This study identified and evaluated the types and differences in VOCs in PL and PT. The established method is simple, rapid, accurate, and sensitive, and it provides theoretical guidance for the identification, tracing, and quality evaluation of PL and PT.

**Keywords:** *Puerariae Lobatae Radix*; *Puerariae Thomsonii Radix*; volatile organic compounds; PCA; OPLS-DA; GC-IMS



**Citation:** Mao, Y.; Zhu, L.; Fu, F.; Zhu, L.; Chen, J.; Liu, J.; Huang, D.; Lei, C. A Comparison of Volatile Organic Compounds in *Puerariae Lobatae Radix* and *Puerariae Thomsonii Radix* Using Gas Chromatography–Ion Migration Spectrometry. *Separations* **2024**, *11*, 31. <https://doi.org/10.3390/separations11010031>

Academic Editors: Rui Miguel Ramos and Cecilia Cagliero

Received: 12 December 2023

Revised: 29 December 2023

Accepted: 11 January 2024

Published: 12 January 2024



**Copyright:** © 2024 by the authors. Licensee MDPI, Basel, Switzerland. This article is an open access article distributed under the terms and conditions of the Creative Commons Attribution (CC BY) license (<https://creativecommons.org/licenses/by/4.0/>).

## 1. Introduction

*Puerariae Lobatae Radix* (PL) and *Puerariae Thomsonii Radix* (PT) are traditional medicinal materials. They are included in the “List of Items Both Food and Drugs” by the Ministry of Health of China, detailing their widespread use in medicine, health products, food, and so on [1,2]. In order to improve their taste, efficacy, and convenience, they are usually eaten in powder form. Although China has formulated systems and regulations for the application of powdered traditional Chinese medicine and food, the application of powdered Chinese medicine faces obstacles. Furthermore, powdered Chinese medicine does not display the obvious characteristics of conventional Chinese medicine, so it is relatively difficult to identify. The authenticity of the powder of traditional Chinese medicine directly affects the safety and efficacy of traditional Chinese medicine, so the scientific identification of the powder of Chinese medicine is very important. PL and PT are derived from the dried roots of leguminous plants *Pueraria lobata* (Willd.) Ohwi and *Puerariathomsonii* Benth., respectively. They can release muscles and subside fever, encourage the production of

body fluids, induce eruptions, and elevate spleen yang to arrest diarrhea [3], and they both contain flavonoids, starch, dietary fiber, and a variety of trace elements and other components. Flavonoids such as puerarin, daidzin, and daidzein have significant effects on improving microcirculation and lowering blood pressure [4]. Dietary fibers such as cellulose and lignin have anti-cancer effects and regulate blood sugar [5]. Starch is the main component of PL and PT, which contains trace isoflavone compounds, which are rich in calcium, phosphorus, potassium, iron, zinc, and other mineral elements essential for the human body [6] and is often used as raw material for new health food [7]. Although PL and PT contain similar components, the content of pueraria is greatly different due to the influence of the growing environment and variety. The 2020 edition of the Chinese Pharmacopoeia stipulates that the contents of puerarin in PL and PT are not less than 2.4% and 0.3%, respectively. Puerarin is a special isoflavone compound in PL and PT that can be used to treat cardiovascular and cerebrovascular diseases [8], diabetes and complications of diabetes [9], osteonecrosis [10], Parkinson's disease [11], Alzheimer's disease [12], endometriosis [13], cancer [14], etc.

Most of the original plants of PL are wild, while most of the original plants of PT are cultivated. At present, there are many cultivated varieties of PL in various places, and the sources of artificially cultivated varieties are complex, resulting in an uneven quality and yield of medicinal materials. In addition, low-cost PT and PL are often mixed and sold to obtain higher profits [15], which seriously affects the safety and effectiveness of drugs [16]. At present, the identification studies of PL and PT mostly adopt trait identification, microscopic identification, high-performance liquid fingerprints [17], gene sequencing [18], etc. Although they are provided more choices for identification, there are also some limitations, such as the character identification is subjective, the microscopic identification is not specific, the HPLC identification operation is cumbersome and time-consuming, and the gene sequencing technology is relatively difficult. Therefore, an efficient, rapid, and intuitive method is urgently needed for the analysis and identification of PL and PT.

Volatile organic compounds (VOCs) are important indicators for the identification and quality evaluation of traditional Chinese medicine. At present, gas chromatography–ion migration spectrometry (GC-IMS) is a new analysis technology for VOC detection that has been widely used in the separation, identification, and quantification of VOCs. It has a high separation capability for GC and fast response, high resolution, and high sensitivity for IMS [19]. In the process of substance analysis, the sample requires limited pretreatment to retain the sample's smell to the maximum extent, and via signal integration in the spectrum, the visualization of flavor substances can be realized, and the types of VOCs in the sample can be rapidly analyzed [20–23]. It has been widely used in the analysis of food flavor [24–29]. He Jia used HS-GC-IMS technology to analyze VOCs in *Ophiopogon* from different producing areas, and these characteristics could effectively identify *Ophiopogon* from Sichuan and Zhejiang, as well as the two traditional main producing areas of Cixi City and Sanmen County, providing a scientific basis for the identification of *Ophiopogon* origin [30]. Zhen–Zhou Wang used GC-IMS technology to identify *Ginseng Radix ET Rhizoma Rubra*, *Panaxis Quniquefolii Radix*, and *Ginseng*, and realized the origin traceability of *Ginseng* via a gas-phase ion migration system combined with data analysis software, providing reference for the identification of *Ginseng* and clinical use accuracy [31]. Fengliu Guo used GC-IMS to identify *Fritillariae Cirrhosae Bulbus* and other *Fritillaria*, providing new ideas and data support for the rapid authenticity identification of *Fritillariae Cirrhosae Bulbus* [32].

At present, there are almost no reports on the identification of PL and PT using GC-IMS. Therefore, in this study, we analyzed and identified the VOCs of PL and PT using GC-IMS technology and established the fingerprints of VOCs. Additionally, the differences between the VOCs of PL and PT were explored by combining principal component analysis (PCA) and orthogonal partial least squares discriminant analysis (OPLS-DA), which provides technical support for VOCs' rapid analysis and the identification of variety for PL and PT.

## 2. Materials and Methods

### 2.1. Materials

The powders of *Puerariae Lobatae Radix* were purchased from the National Institutes for Food and Drug Control, Beijing, China (No. 121551-201805, named PL); *Puerariae Lobatae Radix* is the dried root of *Pueraria lobata* (Willd.) Ohwi, commonly known as “ye ge”.

The powders of *Puerariae Thomsonii Radix* were purchased from Yifeng Pharmacy, Changsha, China (No. 220801, named PT). *Puerariae Thomsonii Radix* is the dried root of *Pueraria thomsonii* Benth., commonly known as “fen ge”.

### 2.2. Analysis Using GC–IMS

PL and PT were ground into powders. After passing through a 65-mesh sieve, 1 g of the powders was accurately weighed into a 20 mL headspace bottle. Then, they were incubated at 80 °C for 20 min, and the samples were injected. Three parallel samples were included for each group.

Headspace sampling conditions: the sample incubation temperature was 80 °C, the incubation speed was 500 r/min, the incubation time was 20 min, the injection volume was 500 µL, the needle temperature was 85 °C, and splitless injection was performed.

Chromatographic conditions: FlavourSpec<sup>®</sup> gas-phase ion mobility spectrometer (G.A.S., Dortmund, Germany); CTC-PAL 3 static headspace automatic sampling device (CTC Analytics AG, Zwingen, Switzerland); 20 mL headspace bottle (Shandong Haineng Scientific Instrument Co., Ltd., Jinan, China); the chromatographic column was MXT-WAX capillary chromatography column (15 m × 0.53 mm × 1 µm, Restek Company of the United States, Bellefonte, PA, USA); temperature: 60 °C; carrier gas: high-purity nitrogen (purity ≥ 99.999%); programmed pressure increase: initial flow rate of 2.00 mL/min maintained for 2 min, linearly increased to 10.00 mL/min, linearly increased to 100.00 mL/min within 10 min, and maintained for 40 min. Chromatography running time: 60 min; injection port temperature: 80 °C.

IMS conditions: drift tube temperature was 45 °C, drift gas was N<sub>2</sub>, and drift gas velocity was 75 mL/min.

### 2.3. Data Analysis

The software configured by GAS company and the built-in NIST gas chromatography retention index database and IMS migration time database were used to characterize the VOCs in the sample. The plug-in of VOCal data processing software, such as Reporter, Gallery Plot, and Dynamic PCA, was used to generate the 3D spectrum, 2D spectrum, difference spectrum, fingerprints, and PCA map of VOCs, respectively, to compare VOCs between samples. SIMCA software was used for OPLS-DA to calculate the projected importance of variables (VIP).

## 3. Results

### 3.1. GC-IMS Analysis of VOCs in PT and PL

GC-IMS was used to analyze the VOCs of PL and PT, and a three-dimensional spectrum was obtained, in which the X axis represents the ion drift time, the Y axis represents the retention time of the gas chromatograph, and the Z axis represents the peak intensity used for quantification, as shown in Figure 1. We can observe the difference in VOCs in the PL and PT samples. To facilitate observation, the following two-dimensional top view is used for comparison. As shown in Figure 2, the horizontal coordinate is ion drift time, the red vertical line at 1.0 is the normalized reactive ion peak (RIP peak), and the vertical coordinate is the retention time of gas chromatography. Each point on either side of the RIP represents a volatile organic compound. The color represents the peak strength of the substance. From blue to red, the darker the color, the greater the peak intensity. There are certain differences in VOCs in PT and PL samples, as can be seen in Figure 2.

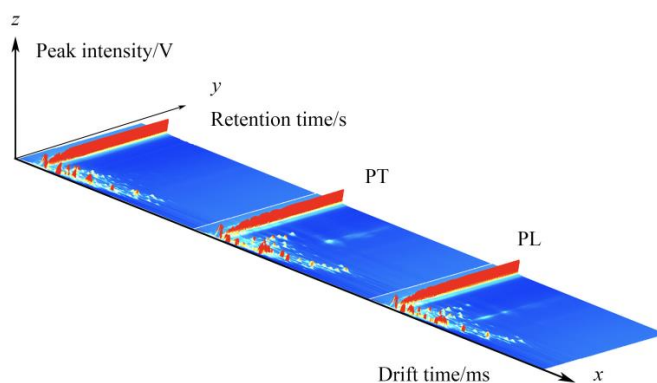


Figure 1. GC-IMS three-dimensional spectrum of PL and PT.

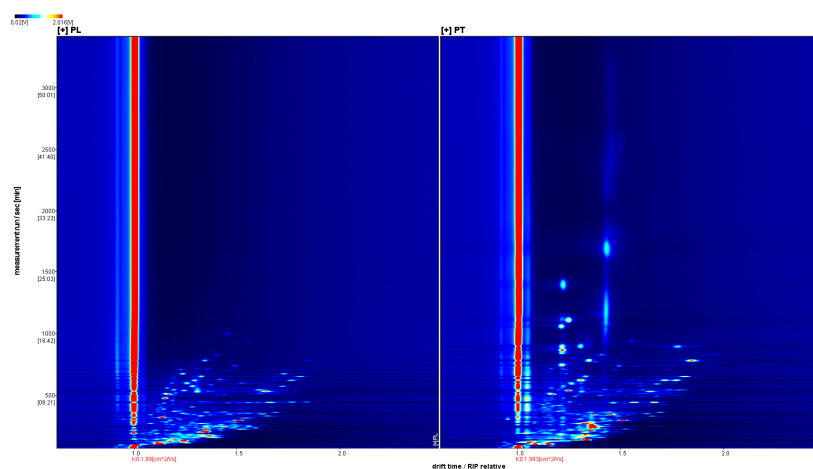


Figure 2. GC-IMS two-dimensional spectrum of PL and PT.

In order to further visually compare the differences in VOCs, the spectra of PL samples were selected as the reference, and the spectra of the PT samples were deducted from the reference ratio to obtain the difference comparison diagram of different samples, as shown in Figure 3. If the two volatile substances are consistent, the deducted background is white, while red means that the concentration of the substance is higher than the reference, and blue means that the concentration of the substance is lower than the reference. It is easier to distinguish the difference between two samples using contrast atlases.

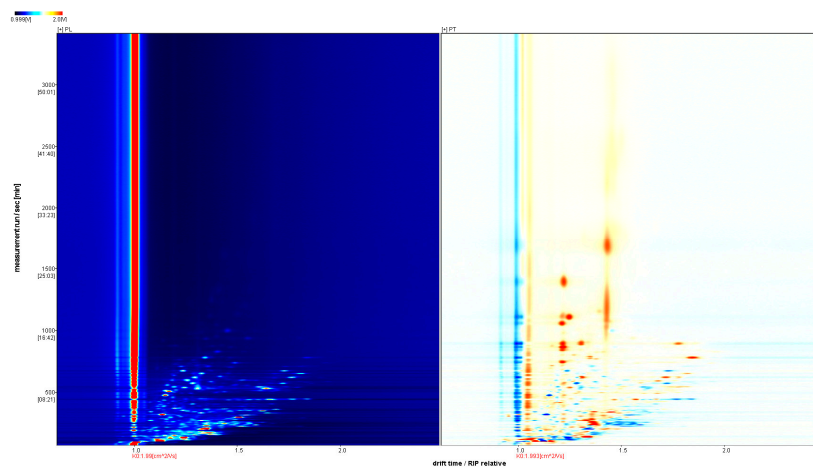
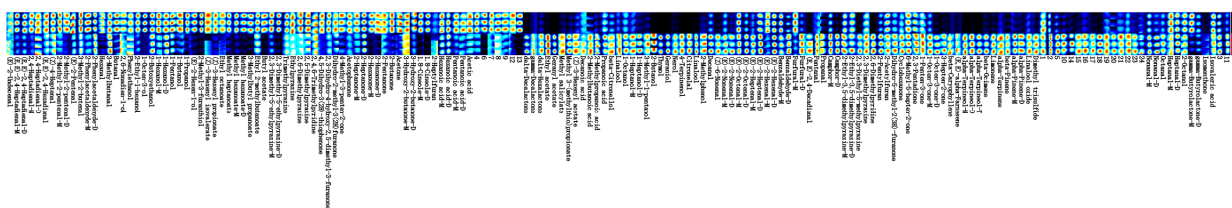


Figure 3. Comparison of GC-IMS differences between PL and PT.

### 3.2. Fingerprints of VOCs in PL and PT

The construction of characteristic flavor fingerprints of PL and PT can provide an effective means for quality evaluation and identification of the variety. To find the exact difference in VOCs between samples of PL and PT, the GC-IMS results of the two samples were further analyzed using the Gallery Plot plug-in, and the VOCs detected in each sample were selected for a fingerprint comparison (Figure 4). Each row in the diagram represents all of the selected signal peaks in the sample, and each column represents the signal peaks of the same volatile organic compound in a different sample. Some substances are followed by M, D, and T, which are monomers, dimers, and trimers of the same substance, respectively. The numbers are unidentified peaks, and the darker the color of each bright spot, the greater the compound content. The complete volatile information for each sample and the differences in volatiles between the samples are outlined in Figure 4.



**Figure 4.** Fingerprints of VOCs in PL and PT.

A comprehensive analysis of Figure 4 showed that the contents of VOCs such as 3-methylbutyraldehyde, 1-octene-3-ol, e-2-hexene-1-ol, isovalerate leaf alcohol ester, butyl acetate, 2,3-dimethyl-5-ethylpyrazine, 2-hexanone, and 1,8-cineulin were high in PL. The contents of VOCs such as delta-decalactone, citronellal, Z-6-nonenal, (E, E)-2, 4-decadienal, camphor,  $\alpha$ -terpinol, and  $\alpha$ -pinene were high in PT.

### 3.3. Identification of VOCs in Different PL and PT

A total of 173 VOCs were detected from PL and PT using GC-IMS analysis, as shown in Table 1. A total of 149 VOCs (monomers, dimers, or trimers) were identified by comparing the NIST2020 vapor phase retention index database built into the practical Vocal software with the IMS migration time database of G.A.S. Among them, there were 38 aldehydes, 22 alcohols, 22 ketones, 19 esters, 13 terpenes, 10 acids, 10 pyrazines, 6 terpenes, 4 furans, and 2 pyridines. In addition, the peak areas of PL and PT show significant differences in the content of VOCs, such as 3-methylbutyraldehyde, 1-octene-3-ol, e-2-hexene-1-ol, isovalerate leaf alcohol ester, butyl acetate, 2,3-dimethyl-5-ethylpyrazine, 2-hexanone, 1,8-cineole, delta-decenolactone, citronellal, Z-6-nonenal, (E, E)-2,4-decenal, camphor, alpha-terpinol,  $\alpha$ -pinene, etc.

**Table 1.** Results of VOC analysis of PL and PT.

Count	Compound	CAS	Molecular Formula	RI	Rt (s)	Dt (RIPrel)	Comment
1	delta-Decalactone	C705862	C <sub>10</sub> H <sub>18</sub> O <sub>2</sub>	1589.8	1686.545	1.43476	
2	Decanoic acid	C334485	C <sub>10</sub> H <sub>20</sub> O <sub>2</sub>	1516.9	1544.131	1.56651	
3	(E)-2-Undecenal	C53448070	C <sub>11</sub> H <sub>20</sub> O	1413.4	1341.792	1.56651	
4	(Z)-3-Hexenyl isovalerate	C35154451	C <sub>11</sub> H <sub>20</sub> O <sub>2</sub>	1238.1	999.416	1.45514	
5	2-Heptylfuran	C3777717	C <sub>11</sub> H <sub>18</sub> O	1215.1	954.414	1.40119	
6	beta-Citronellol	C106229	C <sub>10</sub> H <sub>20</sub> O	1205.2	935.127	1.35083	
7	Decanal	C112312	C <sub>10</sub> H <sub>20</sub> O	1206.2	936.964	1.55586	

Table 1. Cont.

Count	Compound	CAS	Molecular Formula	RI	Rt (s)	Dt (RIPrel)	Comment
8	2,6-Nonadien-1-ol	C7786449	C <sub>9</sub> H <sub>16</sub> O	1174.2	874.511	1.3814	
9	Ethyl octanoate	C106321	C <sub>10</sub> H <sub>20</sub> O <sub>2</sub>	1169.3	864.971	1.47097	
10	(E)-2-Nonenal	C18829566	C <sub>9</sub> H <sub>16</sub> O	1151.6	830.265	1.40739	Monomer
11	(E)-2-Nonenal	C18829566	C <sub>9</sub> H <sub>16</sub> O	1152.2	831.527	1.96372	Dimer
12	Camphor	C76222	C <sub>10</sub> H <sub>16</sub> O	1127.7	783.568	1.34735	Monomer
13	Camphor	C76222	C <sub>10</sub> H <sub>16</sub> O	1128.0	784.199	1.84539	Dimer
14	Phenylethanol	C60128	C <sub>8</sub> H <sub>10</sub> O	1116.4	761.482	1.29436	
15	Nonanal	C124196	C <sub>9</sub> H <sub>18</sub> O	1105.5	740.324	1.49251	Monomer
16	Nonanal	C124196	C <sub>9</sub> H <sub>18</sub> O	1105.5	740.324	1.93345	Dimer
17	Linalool	C78706	C <sub>10</sub> H <sub>18</sub> O	1099.8	729.114	1.20504	
18	2-Ethyl-3,5-dimethylpyrazine	C13925070	C <sub>8</sub> H <sub>12</sub> N <sub>2</sub>	1090.6	710.618	1.23206	Monomer
19	(Z)-3-Hexenyl propionate	C33467742	C <sub>9</sub> H <sub>16</sub> O <sub>2</sub>	1091.9	713.358	1.36119	
20	2-Ethyl-3,5-dimethylpyrazine	C13925070	C <sub>8</sub> H <sub>12</sub> N <sub>2</sub>	1090.6	710.618	1.73805	Dimer
21	1-Octanol	C111875	C <sub>8</sub> H <sub>18</sub> O	1087.9	705.137	1.47079	
22	2,3-Dimethyl-5-ethylpyrazine	C15707343	C <sub>8</sub> H <sub>12</sub> N <sub>2</sub>	1073.2	674.995	1.24107	Monomer
23	2,3-Dimethyl-5-ethylpyrazine	C15707343	C <sub>8</sub> H <sub>12</sub> N <sub>2</sub>	1073.2	674.995	1.73655	Dimer
24	delta-Hexalactone	C823223	C <sub>6</sub> H <sub>10</sub> O <sub>2</sub>	1083.6	696.232	1.15249	
25	(E)-2-Octenal	C2548870	C <sub>8</sub> H <sub>14</sub> O	1062.8	653.758	1.33116	Monomer
26	(E)-2-Octenal	C2548870	C <sub>8</sub> H <sub>14</sub> O	1062.8	653.758	1.81162	Dimer
27	Acetophenone	C98862	C <sub>8</sub> H <sub>8</sub> O	1061.1	650.333	1.19153	
28	2,3-Dihydro-4-hydroxy-2,5-dimethyl-3-furanone	C3658773	C <sub>6</sub> H <sub>8</sub> O <sub>3</sub>	1054.9	637.628	1.19698	
29	2-Ethyl-1-hexanol	C104767	C <sub>8</sub> H <sub>18</sub> O	1051.3	630.284	1.4224	
30	2-Phenylacetaldehyde	C122781	C <sub>8</sub> H <sub>8</sub> O	1036.2	599.333	1.52577	Monomer
31	2-Phenylacetaldehyde	C122781	C <sub>8</sub> H <sub>8</sub> O	1036.5	599.858	1.25729	Dimer
32	Methyl heptanoate	C106730	C <sub>8</sub> H <sub>16</sub> O <sub>2</sub>	1030.3	587.268	1.37645	
33	1.8-Cineole	C470826	C <sub>10</sub> H <sub>18</sub> O	1023.9	574.043	1.28893	Monomer
34	1.8-Cineole	C470826	C <sub>10</sub> H <sub>18</sub> O	1023.9	574.043	1.72454	Dimer
35	Trimethylpyrazine	C14667551	C <sub>7</sub> H <sub>10</sub> N <sub>2</sub>	1016.8	559.507	1.16495	
36	(E,E)-2,4-Heptadienal	C4313035	C <sub>7</sub> H <sub>10</sub> O	1009.7	544.971	1.19845	Monomer
37	(E,E)-2,4-Heptadienal	C4313035	C <sub>7</sub> H <sub>10</sub> O	1009.9	545.49	1.61061	Dimer
38	Hexanoic acid	C142621	C <sub>6</sub> H <sub>12</sub> O <sub>2</sub>	1003.3	531.992	1.31071	Monomer
39	Hexanoic acid	C142621	C <sub>6</sub> H <sub>12</sub> O <sub>2</sub>	1003.3	531.992	1.64244	Dimer
40	2-Pentylfuran	C3777693	C <sub>9</sub> H <sub>14</sub> O	1006.9	539.26	1.24872	
41	2,4-Heptadienal	C5910850	C <sub>7</sub> H <sub>10</sub> O	997.8	520.571	1.20683	Monomer
42	2,4-Heptadienal	C5910850	C <sub>7</sub> H <sub>10</sub> O	998.0	521.09	1.61899	Dimer
43	2,4,6-Trimethylpyridine	C108758	C <sub>8</sub> H <sub>11</sub> N	995.5	516.418	1.15322	
44	6-Methyl-5-hepten-2-one	C110930	C <sub>8</sub> H <sub>14</sub> O	991.0	508.935	1.17184	
45	2-Octanol	C123966	C <sub>8</sub> H <sub>18</sub> O	988.4	504.689	1.44167	
46	1-Octen-3-one	C4312996	C <sub>8</sub> H <sub>14</sub> O	981.4	493.365	1.27916	Monomer
47	1-Octen-3-ol	C3391864	C <sub>8</sub> H <sub>16</sub> O	971.4	477.086	1.15651	
48	4,5-Dihydro-3(2H)-thiophenone	C1003049	C <sub>4</sub> H <sub>6</sub> OS	962.1	461.87	1.19024	
49	Benzaldehyde	C100527	C <sub>7</sub> H <sub>6</sub> O	947.6	438.16	1.14731	Monomer
50	Benzaldehyde	C100527	C <sub>7</sub> H <sub>6</sub> O	947.8	438.514	1.46313	Dimer
51	(E)-2-Heptenal	C18829555	C <sub>7</sub> H <sub>12</sub> O	952.2	445.591	1.66244	Dimer
52	3-Methylbutyl propanoate	C105680	C <sub>8</sub> H <sub>16</sub> O <sub>2</sub>	953.9	448.422	1.84641	
53	Dihydro-5-methyl-2(3H)-furanone	C108292	C <sub>5</sub> H <sub>8</sub> O <sub>2</sub>	940.5	426.482	1.12278	
54	Methyl hexanoate	C106707	C <sub>7</sub> H <sub>14</sub> O <sub>2</sub>	928.4	406.869	1.28653	Monomer
55	Methyl hexanoate	C106707	C <sub>7</sub> H <sub>14</sub> O <sub>2</sub>	928.8	407.425	1.67625	Dimer
56	2,3-Dimethylpyrazine	C5910894	C <sub>6</sub> H <sub>8</sub> N <sub>2</sub>	925.4	401.866	1.12795	
57	2,5-Dimethylpyrazine	C123320	C <sub>6</sub> H <sub>8</sub> N <sub>2</sub>	915.3	385.36	1.11464	
58	Ethylpyrazine	C13925003	C <sub>6</sub> H <sub>8</sub> N <sub>2</sub>	919.9	392.988	1.15016	
59	2,6-Dimethylpyrazine	C108509	C <sub>6</sub> H <sub>8</sub> N <sub>2</sub>	915.2	385.167	1.14652	

Table 1. Cont.

Count	Compound	CAS	Molecular Formula	RI	Rt (s)	Dt (RIPrel)	Comment
60	2-Butoxyethanol	C111762	C <sub>6</sub> H <sub>14</sub> O <sub>2</sub>	907.1	372.015	1.1975	
61	(E,E)-2,4-Hexadienal	C142836	C <sub>6</sub> H <sub>8</sub> O	905.1	368.815	1.12104	
62	Heptanal	C111717	C <sub>7</sub> H <sub>14</sub> O	901.9	363.483	1.35407	Monomer
63	Heptanal	C111717	C <sub>7</sub> H <sub>14</sub> O	901.9	363.483	1.6939	Dimer
64	2-Acetylfuran	C1192627	C <sub>6</sub> H <sub>6</sub> O <sub>2</sub>	903.6	366.327	1.44145	
65	Pentanoic acid	C109524	C <sub>5</sub> H <sub>10</sub> O <sub>2</sub>	897.5	356.374	1.23876	Monomer
66	Pentanoic acid	C109524	C <sub>5</sub> H <sub>10</sub> O <sub>2</sub>	897.3	356.018	1.51063	Dimer
67	2-Heptanone	C110430	C <sub>7</sub> H <sub>14</sub> O	892.9	348.909	1.26061	Monomer
68	Cyclohexanone	C108941	C <sub>6</sub> H <sub>10</sub> O	892.7	348.553	1.46815	
69	2-Heptanone	C110430	C <sub>7</sub> H <sub>14</sub> O	893.4	349.62	1.62351	Dimer
70	(Z)-4-Heptenal	C6728310	C <sub>7</sub> H <sub>12</sub> O	898.6	358.151	1.14288	
71	gamma-Butyrolactone	C96480	C <sub>4</sub> H <sub>6</sub> O <sub>2</sub>	887.8	343.221	1.08341	Monomer
72	gamma-Butyrolactone	C96480	C <sub>4</sub> H <sub>6</sub> O <sub>2</sub>	887.8	343.221	1.29945	Dimer
73	1-Hexanol	C111273	C <sub>6</sub> H <sub>14</sub> O	878.4	333.623	1.32615	Monomer
74	1-Hexanol	C111273	C <sub>6</sub> H <sub>14</sub> O	878.8	333.979	1.64535	Dimer
75	2-Methyl-3-furanthiol	C28588741	C <sub>5</sub> H <sub>6</sub> OS	866.6	321.537	1.13803	
76	Isovaleric acid	C503742	C <sub>5</sub> H <sub>10</sub> O <sub>2</sub>	857.6	312.295	1.2157	
77	(E)-2-Hexen-1-ol	C928950	C <sub>6</sub> H <sub>12</sub> O	862.5	317.271	1.5434	
78	(E)-2-Hexenal	C6728263	C <sub>6</sub> H <sub>10</sub> O	843.7	298.076	1.17808	Monomer
79	(E)-2-Hexenal	C6728263	C <sub>6</sub> H <sub>10</sub> O	844.0	298.431	1.50942	Dimer
80	Ethyl 2-methylbutanoate	C7452791	C <sub>7</sub> H <sub>14</sub> O <sub>2</sub>	849.3	303.763	1.22784	
81	2-Methyl-2-pentenal	C623369	C <sub>6</sub> H <sub>10</sub> O	826.7	280.657	1.16109	Monomer
82	2-Methyl-2-pentenal	C623369	C <sub>6</sub> H <sub>10</sub> O	826.7	280.657	1.49486	Dimer
83	Furfural	C98011	C <sub>5</sub> H <sub>4</sub> O <sub>2</sub>	819.7	273.548	1.08098	Monomer
84	Furfural	C98011	C <sub>5</sub> H <sub>4</sub> O <sub>2</sub>	819.7	273.548	1.33101	Dimer
85	2-Hexanone	C591786	C <sub>6</sub> H <sub>12</sub> O	809.0	262.528	1.19143	Monomer
86	Dihydro-2-methyl-3(2H)furanone	C3188009	C <sub>5</sub> H <sub>8</sub> O <sub>2</sub>	807.9	261.462	1.42567	
87	2-Hexanone	C591786	C <sub>6</sub> H <sub>12</sub> O	809.7	263.239	1.50092	Dimer
88	Butyl acetate	C123864	C <sub>6</sub> H <sub>12</sub> O <sub>2</sub>	805.1	258.618	1.62836	
89	4-Methyl-3-penten-2-one	C141797	C <sub>6</sub> H <sub>10</sub> O	796.4	249.731	1.44267	
90	1-Pentanol	C71410	C <sub>5</sub> H <sub>12</sub> O	767.6	225.559	1.51549	
91	3-Methyl-2-butenal	C107868	C <sub>5</sub> H <sub>8</sub> O	775.7	231.246	1.35164	
92	(E)-2-Pentenal	C1576870	C <sub>5</sub> H <sub>8</sub> O	745.3	209.918	1.35164	
93	3-Hydroxy-2-butanone	C513860	C <sub>4</sub> H <sub>8</sub> O <sub>2</sub>	728.2	197.93	1.07394	Monomer
94	1-Penten-3-one	C1629589	C <sub>5</sub> H <sub>8</sub> O	705.6	182.083	1.32811	
95	2-Pentanone	C107879	C <sub>5</sub> H <sub>10</sub> O	692.3	172.762	1.3669	
96	Propanoic acid	C79094	C <sub>3</sub> H <sub>6</sub> O <sub>2</sub>	701.1	178.976	1.27192	
97	1-Butanol	C71363	C <sub>4</sub> H <sub>10</sub> O	662.0	160.022	1.37359	
98	2,3-Pentadione	C600146	C <sub>5</sub> H <sub>8</sub> O <sub>2</sub>	651.4	155.983	1.29466	
99	3-Methylbutanal	C590863	C <sub>5</sub> H <sub>10</sub> O	638.4	151.011	1.19835	
100	Acetic acid	C64197	C <sub>2</sub> H <sub>4</sub> O <sub>2</sub>	634.4	149.458	1.15019	
101	Butanal	C123728	C <sub>4</sub> H <sub>8</sub> O	620.6	144.175	1.1114	
102	2-Butanone	C78933	C <sub>4</sub> H <sub>8</sub> O	589.7	132.368	1.24517	
103	Acetone	C67641	C <sub>3</sub> H <sub>6</sub> O	525.5	107.821	1.1221	
104	1-Propanol	C71238	C <sub>3</sub> H <sub>8</sub> O	571.8	125.532	1.1114	
105	Ethyl acetate	C141786	C <sub>4</sub> H <sub>8</sub> O <sub>2</sub>	619.7	143.865	1.3348	
106	2-Butanol	C78922	C <sub>4</sub> H <sub>10</sub> O	601.9	137.029	1.33747	
107	2-Methylpropanoic acid	C79312	C <sub>4</sub> H <sub>8</sub> O <sub>2</sub>	788.3	241.431	1.36155	
108	3-Hydroxy-2-butanone	C513860	C <sub>4</sub> H <sub>8</sub> O <sub>2</sub>	729.9	199.173	1.32944	Dimer
109	Pentanal	C110623	C <sub>5</sub> H <sub>10</sub> O	712.6	187.055	1.20638	
110	Propanal	C123386	C <sub>3</sub> H <sub>6</sub> O	517.3	104.714	1.15822	
111	3-Methyl-1-pentanol	C589355	C <sub>6</sub> H <sub>14</sub> O	853.3	307.925	1.30403	
112	2,6-Dimethylpyridine	C108485	C <sub>7</sub> H <sub>9</sub> N	884.9	340.195	1.45516	
113	gamma-Decalactone	C706149	C <sub>10</sub> H <sub>18</sub> O <sub>2</sub>	2242.0	2960.963	1.45582	

Table 1. Cont.

Count	Compound	CAS	Molecular Formula	RI	Rt (s)	Dt (RIPrel)	Comment
114	beta-Caryophyllene	C87445	C <sub>15</sub> H <sub>24</sub>	1960.3	2410.574	1.45774	
115	(E,E)-alpha-Farnesene	C502614	C <sub>15</sub> H <sub>24</sub>	1837.5	2170.534	1.44026	
116	Geranyl acetate	C105873	C <sub>12</sub> H <sub>20</sub> O <sub>2</sub>	1440.1	1394.063	1.22263	
117	(E,E)-2,4-Decadienal	C25152845	C <sub>10</sub> H <sub>16</sub> O	1317.5	1154.45	1.39648	
118	Thymol	C89838	C <sub>10</sub> H <sub>14</sub> O	1294.4	1109.284	1.24831	
119	Geraniol	C106241	C <sub>10</sub> H <sub>18</sub> O	1268.2	1058.254	1.21258	
120	Nerol	C106252	C <sub>10</sub> H <sub>18</sub> O	1228.2	980.031	1.22169	
121	alpha-Terpineol	C98555	C <sub>10</sub> H <sub>18</sub> O	1186.1	897.749	1.21972	Monomer
122	alpha-Terpineol	C98555	C <sub>10</sub> H <sub>18</sub> O	1186.4	898.355	1.30566	Dimer
123	alpha-Terpineol	C98555	C <sub>10</sub> H <sub>18</sub> O	1186.4	898.355	1.78253	Trimer
124	4-Terpinenol	C562743	C <sub>10</sub> H <sub>18</sub> O	1170.9	868.05	1.21804	
125	Citronelal	C106230	C <sub>10</sub> H <sub>18</sub> O	1158.8	844.413	1.21804	
126	Methyl salicylate	C119368	C <sub>8</sub> H <sub>8</sub> O <sub>3</sub>	1174.9	875.93	1.1658	
127	2,3-Diethyl-5-methylpyrazine	C18138040	C <sub>9</sub> H <sub>14</sub> N <sub>2</sub>	1138.3	804.41	1.27364	
128	Linalool	C78706	C <sub>10</sub> H <sub>18</sub> O	1107.9	745.013	1.21804	
129	(Z)-6-Nonenal	C2277192	C <sub>9</sub> H <sub>16</sub> O	1093.7	716.947	1.16944	
130	Linalool oxide	C60047178	C <sub>10</sub> H <sub>18</sub> O <sub>2</sub>	1083.0	695.065	1.2611	
131	2-Methylphenol	C95487	C <sub>7</sub> H <sub>8</sub> O	1067.1	662.538	1.11611	
132	beta-Ocimene	C13877913	C <sub>10</sub> H <sub>16</sub>	1033.1	592.989	1.68091	
133	Limonene	C138863	C <sub>10</sub> H <sub>16</sub>	1025.8	578.047	1.22338	
134	Methyl 3-(methylthio)propionate	C13532188	C <sub>5</sub> H <sub>10</sub> O <sub>2</sub> S	1025.0	576.309	1.60088	
135	Octanal	C124130	C <sub>8</sub> H <sub>16</sub> O	1010.9	547.468	1.42572	
136	alpha-Terpinene	C99865	C <sub>10</sub> H <sub>16</sub>	1011.2	548.163	1.7398	
137	(Z)-3-Hexenyl acetate	C3681718	C <sub>8</sub> H <sub>14</sub> O <sub>2</sub>	1009.1	543.875	1.78589	
138	Dimethyl trisulfide	C3658808	C <sub>2</sub> H <sub>6</sub> S <sub>3</sub>	987.7	503.647	1.29904	
139	1-Heptanol	C111706	C <sub>7</sub> H <sub>16</sub> O	985.3	499.658	1.40408	Monomer
140	1-Octen-3-one	C4312996	C <sub>8</sub> H <sub>14</sub> O	981.8	494.006	1.67918	Dimer
141	(E)-2-Heptenal	C18829555	C <sub>7</sub> H <sub>12</sub> O	952.9	446.797	1.25569	Monomer
142	beta-Pinene	C127913	C <sub>10</sub> H <sub>16</sub>	971.6	477.383	1.22734	
143	1-Heptanol	C111706	C <sub>7</sub> H <sub>16</sub> O	985.5	499.99	1.77422	Dimer
144	3-Hepten-2-one	C1119444	C <sub>7</sub> H <sub>12</sub> O	935.4	418.205	1.204	
145	alpha-Pinene	C80568	C <sub>10</sub> H <sub>16</sub>	939.9	425.519	1.30737	Monomer
146	alpha-Pinene	C80568	C <sub>10</sub> H <sub>16</sub>	940.3	426.184	1.68418	Dimer
147	2-Methylbutanoic acid	C116530	C <sub>5</sub> H <sub>10</sub> O <sub>2</sub>	870.2	325.194	1.22302	
148	Isomenthone	C491076	C <sub>10</sub> H <sub>18</sub> O	1149.4	826.025	1.33262	
149	Hexanal	C66251	C <sub>6</sub> H <sub>12</sub> O	799.2	252.51	1.56289	

### 3.4. Chemometrics Analysis

#### 3.4.1. PCA of VOCs in Samples

Principal component analysis (PCA) is a multi-variable data analysis tool that converts and reduces the dimensions of the information collected by the sensor to obtain the most important factor with the largest contribution rate, and it reflects the difference in the test samples on the PCA diagram [33]. In order to distinguish the difference between PL and PT, PCA was performed on all samples of PL and PT. As shown in Figure 5, there are clear differences between PL and PT. If the distance between the samples is close then the difference is small. If the distance is long then the difference is obvious. As can be seen from Figure 5, the distance between PL and PT is very long, which means that the VOC contents of them are significantly different.

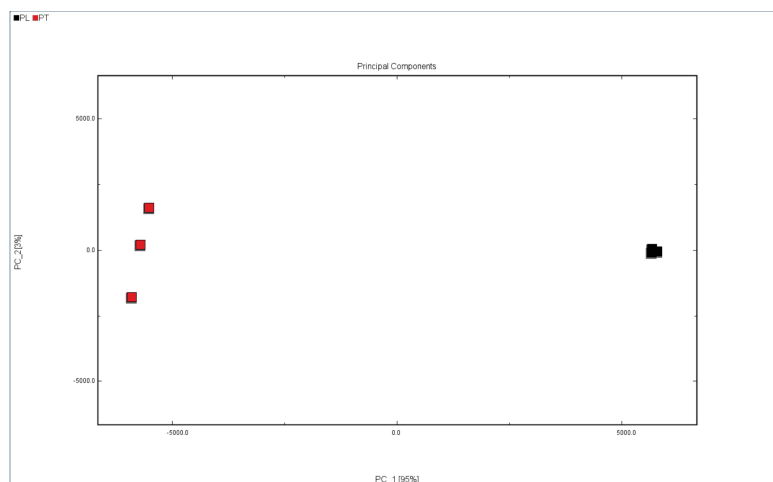


Figure 5. PCA analysis of PL and PT.

### 3.4.2. Orthogonal Partial Least Squares Discriminant Analysis (OPLS-DA)

PCA focuses on describing the classification trend of samples. Unlike PCA analysis, OPLS-DA is a supervised analysis that can statistically analyze complex data dimensionality reduction, visualize the data, and then build a model to predict the data. In order to further explore and judge the differences and accuracy of VOCs in PL and PT, we further evaluated the feasibility of GC-IMS technology for rapid authenticity identification. The peak volume of 149 VOCs with large differences in selected content was taken as a variable, and the OPLS-DA scores were obtained with partial least squares discriminant analysis. The results are shown in Figure 6, which are consistent with the results of PCA, and different Pueraria samples are clearly distinguished. According to the data processed by SIMCA software, the model can relatively accurately summarize, explain, and predict; the VOC composition of PL and PT is identifiable according to this study; and different varieties can be distinguished to clarify the differences between PL and PT. Figure 6 shows the verification of the OPLS-DA model by using permutation testing. It can be seen from Figure 7 that  $R^2$  intersects the vertical axis (0, 0.842),  $Q^2$  intersects the vertical axis (0, 0.0186), and the slope of the two regression lines is large. It was confirmed that the model could be used to study the classification and discrimination of VOCs in two different varieties of PL and PT via verification.

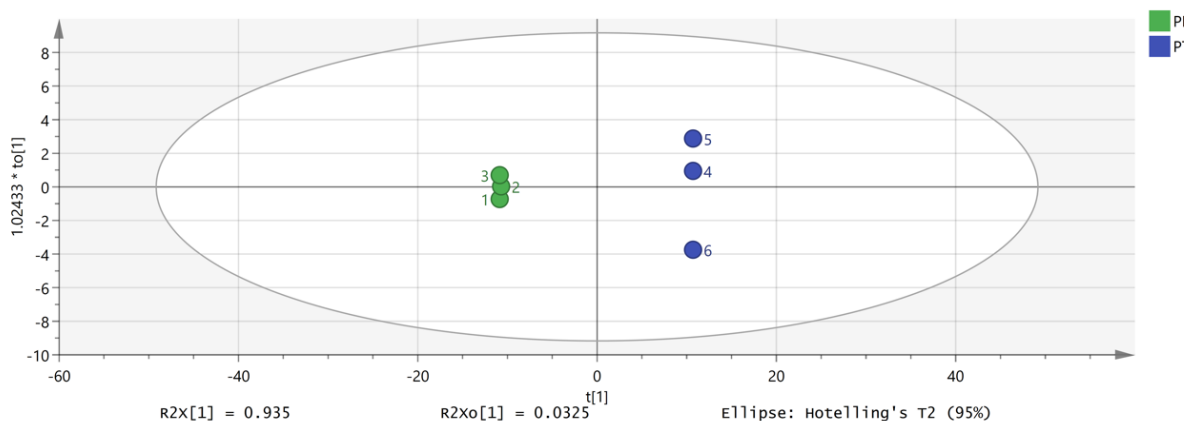


Figure 6. OPLS-DA analysis of VOCs in PT and PL.

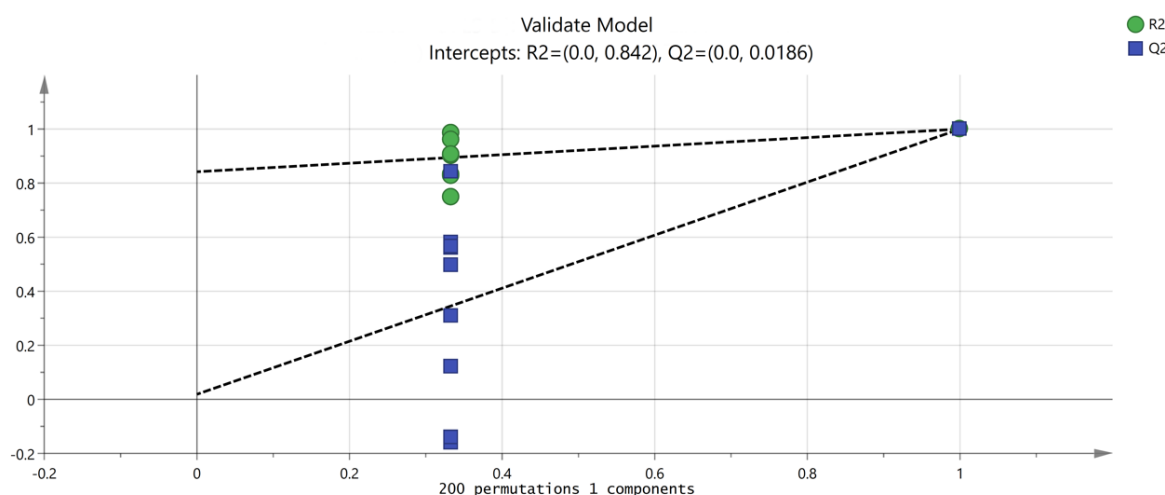


Figure 7. Permutation test results of VOCs in PT and PL.

The variable importance projection (VIP) of the OPLS-DA model with different peak volumes of VOCs is highlighted in Figure 8. The larger the VIP value, the more significant the difference. By observing the VIP value, potential markers can be analyzed. The results showed that there were five VOCs with a VIP value > 1 and  $p < 0.05$ , including 2-methyl-3-furanthiol, 1-propanol, ethyl acetate, gamma-butyrolactone-M, and methyl hexanoate-D. The above five VOCs are important indicators for the classification and identification of PL and PT, and they can provide a reference for the rapid authenticity identification of the two pieces.

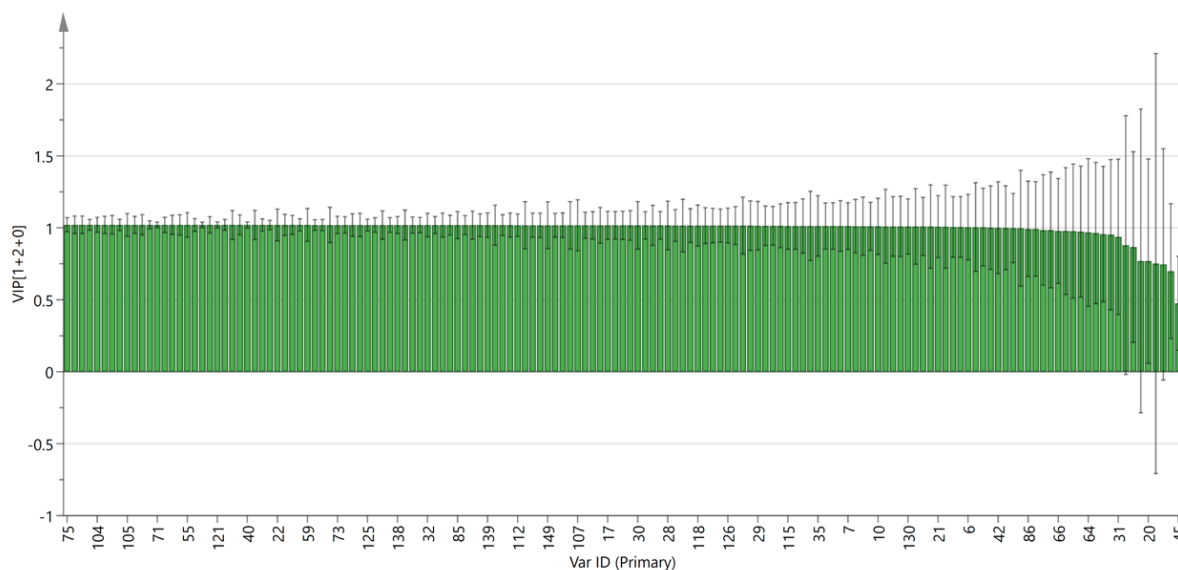


Figure 8. VIP value of the characteristic variables.

#### 4. Discussion

In this study, we used GC-IMS for the first time to analyze and identify VOCs in PL and PT. A total of 173 VOCs were detected, and 149 of them were identified, mainly including aldehydes, alcohols, ketones, lipids, and other components, by rapidly comparing the types and contents of VOCs in PL and PT by observing the size and color changes in the sample points representing compound information. By constructing GC-IMS fingerprints, it was shown that the VOCs of PL and PT have extremely high similarity, but the content differences between the groups are obvious. Using principal component analysis and partial least squares discrimination, the distribution of VOCs of PL and PT samples occupies a

relatively independent space in the diagram, which can be easily distinguished. Then, the VIP value and  $p$ -value were used to identify five different markers of PL and PT, which provided a scientific basis for rapid identification. Compared with traditional analytical methods such as enthrone colorimetry and high-performance liquid chromatography for the identification of PL and PT, GC-IMS technology has great room for the development of identifying the origin of Chinese medicinal materials and counterfeit and shoddy materials. Not only can the composition differences in VOCs of Chinese medicinal materials be analyzed, but samples with similar compositions of VOCs can also be accurately classified according to the content differences in characteristic volatile substances. The experimental results of this study show that GC-IMS can effectively analyze and identify the VOCs in PL and PT, detect the difference between PL and PT, and reach scientific judgments. Moreover, this method requires less sample dosage and is simple in the process of drug pretreatment, which has great application potential, and it provides a scientific basis for the research and development of PT and PL identification in the future.

## 5. Conclusions

The rapid identification of traditional Chinese medicines based on “odor” information is an important part of the traditional identification method of traditional Chinese medicines [34]. For example, Houduyuan Cordata has a strong fishy smell, and Xiangjiapi has a special fragrance. Experienced pharmacists can directly and quickly identify authenticity and even evaluate quality based on the unique smell and odor thickness of traditional Chinese medicine. With its fast and convenient advantages, up until now, this method has spread as a traditional identification approach. However, for some decoction pieces with insufficient odor information or even weak odor, it may be difficult to quickly realize the identification of traditional Chinese medicine using the traditional “sniffing” method. As a trace detection technology for VOCs, GC-IMS technology cleverly combines the advantages of the rapid identification of traditional traits with the accuracy and quantification of modern instrument analysis. It can be used to quickly and accurately detect information on VOCs in traditional Chinese medicine to allow the inheritance and development of traditional skills. At present, this technology is widely used in food, agriculture, medicine, and other fields. It is mainly used for the rapid detection and characterization of VOCs in samples, as well as the comparative analysis of the differences in VOCs in different samples, and many studies have shown that GC-IMS technology can be used for the identification or classification of two/multiple types of samples [35,36].

**Author Contributions:** Conceptualization, Y.M. and L.Z. (Lingfeng Zhu); methodology, Y.M. and L.Z. (Lingfeng Zhu); software, F.F. and L.Z. (Lijun Zhu); validation, J.C. and J.L.; formal analysis, Y.M. and L.Z. (Lingfeng Zhu); investigation, L.Z. (Lijun Zhu); resources, J.C.; data curation, J.L.; writing—original draft preparation, Y.M. and L.Z. (Lingfeng Zhu); writing—review and editing, C.L.; visualization, Y.M. and L.Z. (Lingfeng Zhu); supervision, F.F.; project administration, D.H.; funding acquisition, C.L. All authors have read and agreed to the published version of the manuscript.

**Funding:** This research was funded by the Hunan Agricultural Science and Technology Innovation Fund Project, Hunan Academy of Agricultural Sciences (No. 2023CX30) and the First-Class Discipline Project on Chinese Medicine of Hunan University of Chinese Medicine, Hunan University of Chinese Medicine (No. 2023).

**Data Availability Statement:** This published article includes all data generated or analyzed during this study.

**Conflicts of Interest:** The authors declare no conflicts of interest.

## References

1. Gudeta, W.F.; Igori, D.; Belete, M.T.; Kim, S.E.; Moon, J.S. Complete genome sequence of pueraria virus A, a new member of the genus Caulimovirus. *Arch. Virol.* **2022**, *6*, 1481–1485. [[CrossRef](#)] [[PubMed](#)]
2. Wang, S.; Zhang, S.; Wang, S.; Gao, P.; Dai, L. A comprehensive review on Pueraria: Insights on its chemistry and medicinal value. *Biomed. Pharmacother.* **2020**, *131*, 110734. [[CrossRef](#)] [[PubMed](#)]

3. Committee for the National Pharmacopoeia of P.R. China. *Pharmacopoeia of P.R. China, Part I*; Beijing Chemical Industry Press: Beijing, China, 2020.
4. Wu, W.T.; Guo, Z.L.; Ge, S.C.; Kuang, W.L.; Li, W.D.; Wang, S.D.; Liu, P.; Zhou, Z.W.; Zhu, W.F. Pharmacokinetics, pharmacodynamics, and tissue distribution of oral co-loaded puerarin/daidzein mixed micelles in rats. *Chin. J. Chin. Mater. Med.* **2023**, *18*, 5068–5077. [[CrossRef](#)]
5. Ding, Z.E.; Wan, X.C. Extraction and separation of dietary fiber from Pueraria. *J. Cereals Oils* **2004**, *4*, 38–41. [[CrossRef](#)]
6. Liu, D.; Ma, L.; Zhou, Z.; Liang, Q.; Xie, Q.; Ou, K.; Liu, Y.; Su, Y. Starch and mineral element accumulation during root tuber expansion period of Pueraria thomsonii Benth. *Food Chem.* **2021**, *343*, 128445. [[CrossRef](#)]
7. Zhang, J.J.; Chen, M.Q.; JIN, L.B.; Yang, H.L. Research progress of pueraria starch. *Guangxi J. Light Ind.* **2010**, *2*, 4–5. [[CrossRef](#)]
8. Zhou, Y.X.; Zhang, H.; Peng, C. Puerarin: A review of pharmacological effects. *Phytother. Res.* **2014**, *7*, 961–975. [[CrossRef](#)]
9. Bai, Y.L.; Han, L.L.; Qian, J.H.; Wang, H.Z. Molecular Mechanism of Puerarin Against Diabetes and its Complications. *Front. Pharmacol.* **2022**, *12*, 780419. [[CrossRef](#)]
10. Tang, W.; Xiao, L.; Ge, G.; Zhong, M.; Zhu, J.; Qin, J.; Feng, C.; Zhang, W.; Bai, J.; Zhu, X.; et al. Puerarin inhibits titanium particle-induced osteolysis and RANKL-induced osteoclastogenesis via suppression of the NF- $\kappa$ B signaling pathway. *J. Cell Mol. Med.* **2020**, *20*, 11972–11983. [[CrossRef](#)]
11. Zhu, G.; Wang, X.; Wu, S.; Li, X.; Li, Q. Neuroprotective effects of puerarin on 1-methyl-4-phenyl-1,2,3,6-tetrahydropyridine induced Parkinson's disease model in mice. *Phytother. Res.* **2014**, *2*, 179–186. [[CrossRef](#)]
12. Hong, X.P.; Chen, T.; Yin, N.N.; Han, Y.M.; Yuan, F.; Duan, Y.J.; Shen, F.; Zhang, Y.H.; Chen, Z.B. Puerarin Ameliorates D-Galactose Induced Enhanced Hippocampal Neurogenesis and Tau Hyperphosphorylation in Rat Brain. *J. Alzheimers. Dis.* **2016**, *2*, 605–617. [[CrossRef](#)] [[PubMed](#)]
13. Yu, J.; Zhao, L.; Zhang, D.Y.; Zhai, D.X.; Shen, W.; Bai, L.L.; Liu, Y.Q.; Cai, Z.L.; Li, J.; Yu, C.Q. The effects and possible mechanisms of puerarin to treat endometriosis model rats. *Evid. Based Complement. Altern. Med.* **2015**, *2015*, 269138. [[CrossRef](#)] [[PubMed](#)]
14. Hu, Y.; Li, X.; Lin, L.; Liang, S.; Yan, J. Puerarin inhibits non-small cell lung cancer cell growth via the induction of apoptosis. *Oncol. Rep.* **2018**, *4*, 1731–1738. [[CrossRef](#)] [[PubMed](#)]
15. Wei, F.; Liu, W.; Yan, H.; Shi, Y.; Zhang, W.J.; Zhang, P.; Cheng, X.L.; Ma, S.C. Analysis of quality and related problems of Chinese medicinal materials and decoction pieces. *Chin. J. Pharm. Sci.* **2015**, *4*, 277–283. [[CrossRef](#)]
16. Xiang, G.; Zhou, L.P.; Gui, J.X.; Zhu, J.X. Research progress and prospect of near infrared spectroscopy in consumer products. *Infrared* **2017**, *12*, 1–5+12. [[CrossRef](#)]
17. Jiang, R.W.; Lau, K.M.; Lam, H.M.; Yam, W.S.; Leung, L.K.; Choi, K.L.; Waye, M.M.; Mak, T.C.; Woo, K.S.; Fung, K.P. A comparative study on aqueous root extracts of Pueraria thomsonii and Pueraria lobata by antioxidant assay and HPLC fingerprint analysis. *J. Ethnopharmacol.* **2005**, *96*, 133–138. [[CrossRef](#)]
18. Li, J.; Yang, M.; Li, Y.; Jiang, M.; Liu, C.; He, M.; Wu, B. Chloroplast genomes of two Pueraria DC. species: Sequencing, comparative analysis and molecular marker development. *FEBS Open Bio* **2022**, *12*, 349–361. [[CrossRef](#)]
19. He, S.; Zhang, B.; Dong, X.; Wei, Y.; Li, H.; Tang, B. Differentiation of Goat Meat Freshness Using Gas Chromatography with Ion Mobility Spectrometry. *Molecules* **2023**, *9*, 3874. [[CrossRef](#)]
20. Zhou, S.; Feng, D.; Zhou, Y.; Duan, H.; He, Y.; Jiang, Y.; Yan, W. Characteristic Volatile Organic Compound Analysis of Different Cistanches Based on HS-GC-IMS. *Molecules* **2022**, *27*, 6789. [[CrossRef](#)]
21. Augustini, A.L.R.M.; Borg, C.; Sielemann, S.; Telgheder, U. Making Every Single Puff Count—Simple and Sensitive E-Cigarette Aerosol Sampling for GCxIMS and GC-MS Analysis. *Molecules* **2023**, *28*, 6574. [[CrossRef](#)]
22. Feng, D.; Wang, J.; He, Y.; Ji, X.J.; Tang, H.; Dong, Y.M.; Yan, W.J. HS-GC-IMS detection of volatile organic compounds in Acacia honey powders under vacuum belt drying at different temperatures. *Food Sci. Nutr.* **2021**, *9*, 4085–4093. [[CrossRef](#)]
23. Li, M.; Yang, R.; Zhang, H.; Wang, S.; Chen, D.; Lin, S. Development of a flavor fingerprint by HS-GC-IMS with PCA for volatile compounds of Tricholoma matsutake Singer. *Food Chem.* **2019**, *290*, 32–39. [[CrossRef](#)] [[PubMed](#)]
24. Wang, S.; Chen, H.; Sun, B. Recent progress in food flavor analysis using gas chromatography-ion mobility spectrometry (GC-IMS). *Food Chem.* **2020**, *15*, 126158. [[CrossRef](#)]
25. Yuan, J.; Li, H.; Cao, S.; Liu, Z.; Li, N.; Xu, D.; Mo, H.; Hu, L. Monitoring of Volatile Compounds of Ready-to-Eat Kiwifruit Using GC-IMS. *Foods* **2023**, *12*, 4394. [[CrossRef](#)]
26. Calle, J.L.P.; Vázquez-Espinosa, M.; Barea-Sepúlveda, M.; Ruiz-Rodríguez, A.; Ferreiro-González, M.; Palma, M. Novel Method Based on Ion Mobility Spectrometry Combined with Machine Learning for the Discrimination of Fruit Juices. *Foods* **2023**, *12*, 2536. [[CrossRef](#)] [[PubMed](#)]
27. Ruiz, M.J.; Salatti-Dorado, J.A.; Cardador, M.J.; Frizzo, L.; Jordano, R.; Arce, L.; Medina, L.M. Relationship between Volatile Organic Compounds and Microorganisms Isolated from Raw Sheep Milk Cheeses Determined by Sanger Sequencing and GC-IMS. *Foods* **2023**, *12*, 372. [[CrossRef](#)]
28. Wu, D.; Xia, Q.; Cheng, H.; Zhang, Q.; Wang, Y.; Ye, X. Changes of Volatile Flavor Compounds in Sea Buckthorn Juice during Fermentation Based on Gas Chromatography–Ion Mobility Spectrometry. *Foods* **2022**, *11*, 3471. [[CrossRef](#)] [[PubMed](#)]
29. Jiang, H.; Duan, W.; Zhao, Y.; Liu, X.; Wen, G.; Zeng, F.; Liu, G. Development of a Flavor Fingerprint Using HS-GC-IMS for Volatile Compounds from Steamed Potatoes of Different Varieties. *Foods* **2023**, *12*, 2252. [[CrossRef](#)]
30. He, J.; Ye, L.; Li, J.; Huang, W.; Huo, Y.; Gao, J.; Liu, L.; Zhang, W. Identification of Ophiopogonis Radix from different producing areas by headspace-gas chromatography-ion mobility spectrometry analysis. *J. Food Biochem.* **2022**, *6*, e13850. [[CrossRef](#)]

31. Huang, J.; Ding, S.; Xiong, S.; Liu, Z. The Mediating Effects of Diabetes Distress, Anxiety, and Cognitive Fusion on the Association Between Neuroticism and Fear of Hypoglycemia in Patients with Type 2 Diabetes. *Front. Psychol.* **2021**, *12*, 697051. [[CrossRef](#)]
32. Hapunda, G.; Abubakar, A.; Pouwer, F.; Vijver, F. Correlates of fear of hypoglycemia among patients with type 1 and 2 diabetes mellitus in outpatient hospitals in Zambia. *Int. J. Diabetes Dev. Ctries.* **2020**, *4*, 619–626. [[CrossRef](#)]
33. Zhang, Q.; Ding, Y.C.; Gu, S.Q.; Zhu, S.C.; Zhou, X.X.; Ding, Y.T. Identification of changes in volatile compounds in dry-cured fish during storage using HS-GC-IMS. *Food Res. Int.* **2020**, *137*, 109339. [[CrossRef](#)] [[PubMed](#)]
34. Lu, Y. *Research on Rapid Identification of TCM Decoction Pieces Based on "Odor" Information Analysis*; Chengdu University of Traditional Chinese Medicine: Chengdu, China, 2017.
35. Liang, T.Y.; Juan, Y.; Hao, D.; Yu, L.M.; Bing, H.; Zeng, X.F. Identification of volatile flavor compounds in Different years of Xinhui orange peel based on GC-IMS. *Chin. Condiments* **2020**, *4*, 168–173. [[CrossRef](#)]
36. Yang, B.Y.; Yao, L.; Ji, H.Y.; Jing, Y.Y.; Chen, G.L.; Gang, Z.; Yan, Y.G.; Hu, B.X.; Liang, P. Analysis on the difference of volatile organic compounds VOCs of coltsl nectar before and after moxibustion based on HS-GC-IMS technique. *Chin. Herb. Med.* **2022**, *6*, 1854–1861.

**Disclaimer/Publisher's Note:** The statements, opinions and data contained in all publications are solely those of the individual author(s) and contributor(s) and not of MDPI and/or the editor(s). MDPI and/or the editor(s) disclaim responsibility for any injury to people or property resulting from any ideas, methods, instructions or products referred to in the content.